

# We are IntechOpen, the world's leading publisher of Open Access books Built by scientists, for scientists

6,900

Open access books available

185,000

International authors and editors

200M

Downloads

Our authors are among the

154

Countries delivered to

TOP 1%

most cited scientists

12.2%

Contributors from top 500 universities



WEB OF SCIENCE™

Selection of our books indexed in the Book Citation Index  
in Web of Science™ Core Collection (BKCI)

Interested in publishing with us?  
Contact [book.department@intechopen.com](mailto:book.department@intechopen.com)

Numbers displayed above are based on latest data collected.  
For more information visit [www.intechopen.com](http://www.intechopen.com)



---

# An Overview of the Establishment of Methodology to Analyse up to 5g-Sample by $k_0$ -Instrumental Neutron Activation Analysis, at CDTN, Brazil

---

Maria Ângela de B.C. Menezes and  
Radojko Jaćimović

Additional information is available at the end of the chapter

<http://dx.doi.org/10.5772/intechopen.83812>

---

## Abstract

The team of the Laboratory for Neutron Activation Analysis, Brazil, has been continuously improving the  $k_0$ -instrumental neutron activation analysis, the  $k_0$ -INAA method, having Jožef Stefan Institute, Slovenia, as partner researcher of the neutron activation technique. The group aims at answering the analytical requests of customers and the needs of the researches developed by the lab. The latest improvement was to establish a methodology to analyse up to 5 g-samples. The usual procedure in neutron activation analysis is to determine elemental concentrations in small samples of about 200 mg, a geometrical point source. The reason why these samples are used is that this geometry brings about a number of simplifications during irradiation and gamma spectrometry. This paper describes the steps carried out in the development of the large sample methodology that has already been published elsewhere and has been applied successfully. The results of some reference materials and samples are displayed. It is important to mention that this research has confirmed that any other laboratory applying  $k_0$ -INAA is able to establish this methodology without having to modify its facilities, since the neutron self-shielding, gamma attenuation, and detector efficiency over the volume source are established.

**Keywords:**  $k_0$ -instrumental neutron activation analysis, large sample, detector efficiency, neutron self-shielding, gamma-ray attenuation

---

## 1. Introduction

When an analytical result is available, several tasks had been accomplished before such as the routine procedure establishment, calibration of instruments, quality assurance and quality

control (QA/QC), training of technical group, good laboratory practice and others. All of these requirements are needed to meet the demand for analytical values that are even increasing in all fields, contributing to environmental monitoring, individual and population health and economical decisions. According to the development of human knowledge, the requirements for quality have been diversified and increasing in several fields. Therefore, the demand for analytical data with smaller uncertainties and lower detection limits is expanding and more requirements are necessary to meet the quality required by the clients.

The nuclear analytical technique, NAA [1, 2], fulfils several requirements. It is well-known that NAA requires a non-chemical preparation—a non-destructive technique—and analyses a large number of elements simultaneously. Besides, it is a traceable technique [3, 4]. It presents sensitivity, multi-element ability, selectivity and versatility and determines chemical elements with precision and accuracy [5, 6]. That is why it is a powerful technique.

The technique is well established at the Laboratory for Neutron Activation Analysis, LNAA, located at the Nuclear Technology Development Centre (CDTN) sponsored by the Brazilian Commission for Nuclear Energy (CNEN), in Belo Horizonte, capital of the Brazilian state of Minas Gerais. The nuclear research reactor, the 100 kW TRIGA MARK I IPR-R1, has enabled the NAA to be applied determining the elemental concentration of different samples, such as soil, sediment, plants, food, medicines and biological tissues of humans and animals, among others [7–20]. The NAA has been applied through relative and parametric methods and has been applied meeting requests of customers both of CDTN and at industries, universities and other institutions. The technique has also been applied in researches of the LNAA. The standardised  $k_0$ -method [21] was established in 1995, being the most efficient form of application of this nuclear analytical technique [8, 9]. The  $k_0$ -method has been continuously improving along its nuclear data [22, 23], which can be found in the form of an Excel file, the  $k_0$ -database 2015 [24].

## 2. Small samples versus large samples

The usual procedure in NAA is to analyse a sample whose mass is lower than 500 mg, considering it as a geometrical point source. This entails a number of simplifications during irradiation and gamma spectrometry [25, 26]. This way, several simplifications can be made such as disregarding the neutron self-shielding, neutron-flux gradients over the sample and self-attenuation of gamma rays. The impact to the accuracy of the results is negligible.

On the other hand, there is a growing demand for the NAA established at CDTN to explore its potential in order to overcome the main limitations when analysing point samples, which are: to reach lower detection limits than those currently in use (for instance in food samples, plants, medicines and lichens) and to carry on analysis at lower cost, that is, to analyse a smaller number of samples and shorter time of analysis. For example, instead of analysing 20 small samples, a single about 4 g composite sample could be analysed; to provide greater representativeness of samples of non-homogeneous materials, for instance, industrial waste materials; to enable the analysis of whole parts in which it is not possible or permitted to remove an

aliquot for analysis, for example, of archaeological ceramics. In addition, the low neutron flux of a low-power reactor can be compensated by increasing the amount of sample to be exposed to irradiation.

A possibility to overcome these problems is to analyse larger samples—samples of more than 0.5 g [25–32]. In order to obtain reliable analysis results, some parameters should be determined: (i) detector efficiency evaluation over the volume source, (ii) neutron flux depression due to absorption and scattering and (iii) the relative attenuation of gamma rays originating from different positions within the sample.

During the irradiation, the neutron field is perturbed during absorption and scattering inside the sample. It is called neutron self-shielding. This can be overcome by experimentally determining the neutron flux distribution in real samples in a defined volume for a matrix [6, 33, 34]. The degree of gamma self-attenuation depends on a number of factors such as sample geometry, linear attenuation coefficient, material density, sample composition and photon energy [35].

The laboratories that have been applying the neutron activation to large samples (LS-INAA) analyse samples in a range of kilogrammes, and for this procedure, special facilities are required, for the activation as well as for the detection. For instance, in Delft, The Netherlands, a facility was built to irradiate and measure samples from 2 to 50 kg [3, 26–31].

### 3. Development of the methodology applied at CDTN

The LNAA determines chemical elemental concentrations following the usual procedure—small cylindrical samples. The irradiations are carried out in the carousel facility of the TRIGA MARK I IPR-R1 reactor that operates at 100 kW with an average thermal neutron flux of  $6.3 \times 10^{11} \text{ cm}^{-2} \text{ s}^{-1}$ . The laboratory has a high demand of analysis, answering the clients' request, analysing several kinds of samples. It is often necessary to overcome the difficulties due to low neutron fluency, inhomogeneity of unknown sample and time consumption of analysis. For that reason, to analyse larger samples would be an attractive possibility. However, it is not allowed to change the infrastructure of irradiation; therefore, a study was developed to verify the possibility to analyse 5 g-samples, maximum mass content in the irradiation vial, 25 times larger than usual samples analysed. The  $k_0$ -method of neutron activation analysis [21] would be applied and the current infrastructure for irradiation and gamma spectrometry facilities would be used. To develop this study, the mass of the small sample analysed was around 200 mg and the larger cylindrical sample, around 5 g.

Aiming at solving the main limitations when dealing with small samples and exploring a new possibility of analysis, a methodology of analysing larger samples or cylindrical samples was established in LNAA at CDTN [16, 36, 37]. All experiments were developed in geological matrix. The reason was that matrix is the one most used in routine elemental analysis at CDTN. All irradiations were performed in the carousel facility of the 100 kW TRIGA MARK I IPR-R1 reactor under an average thermal neutron flux of  $6.3 \times 10^{11} \text{ cm}^{-2} \text{ s}^{-1}$  and average

spectral parameters  $f$  (thermal to epithermal ratio neutron fluxes) and  $\alpha$  (the epithermal flux distribution parameter), 22.67 and 0.0026, respectively. The induced activities were measured on absolutely calibrated HPGe detectors [9]. The vials were inserted in a polystyrene container for irradiation during 8 hours.

Gamma spectroscopy was carried out after suitable decay on an absolute calibrated HPGe detector named D4, GC 5019, CANBERRA, with 50% relative efficiency. The absolute calibration was done following a recommended procedure in the  $k_0$ -standardisation method [6, 9, 21].

The HyperLab programme [38] was used for peak area deconvolution and the software package Kayzero for Windows<sup>®</sup> [39], also called KayWin, was applied. It is a specific programme to calculate the elemental concentration for the so-called small samples—routine procedure—including the efficiency and coincidence correction calculations. It also calculates the values of efficiency for each energy based on the experimental full-energy peak efficiency determined previously for point-source geometry aiming at point sample analysis. This software determines the reference full-energy peak efficiency,  $\varepsilon_p$ , of the detector [9].

The main experimental steps carried out to establish the methodology based on Menezes and Jaćimović [16] and Menezes et al. [36, 37] will be described. Some tables and figures related to the development have already been published and are shown here with permission. However, other tables are original.

To establish the methodology to analyse a large sample, it was necessary to check three parameters: (i) detector efficiency over the volume source, (ii) neutron self-shielding during neutron irradiation and (iii) gamma-ray attenuation within the sample during counting [26, 35, 40].

### 3.1. Detector efficiency over the volume source

To evaluate the detector efficiency over the volume of the sample applying the  $k_0$ -method, using the KayWin software, it is necessary to determine the reference full-energy peak efficiency,  $\varepsilon_p$ . This programme calculates the elemental concentration for small samples—routine procedure—while calculating the efficiency and coincidence correction. The values of efficiency for each energy are also calculated based on the experimental full-energy peak efficiency. This efficiency was determined previously for point-source geometry aiming at point sample analysis. It is necessary to provide the detector characteristics, container and geometry dimensions, composition of the sample and reference efficiency curve to determine its efficiency. The final calculations will give the full-energy peak efficiency,  $\varepsilon_p$ , and the effective solid angle ( $\overline{\Omega}_{eff}$ ).

The KayWin software calculates, for each gamma energy in a spectrum, the efficiency, when the elemental concentration of a real sample is determined. The detector efficiency can also be determined by ANGLE V3.0 software [41] that was successfully installed at CDTN. This software is specific to calculate the full-energy peak efficiency of the semiconductor detector to several source geometries as point and cylindrical shapes, Marinelli, etc. In this study, it was



used to validate the full-energy peak efficiency,  $\varepsilon_p$ , calculated by KayWin. Both software need information on the detector characteristics, container and geometry dimensions, composition of the sample and reference efficiency curve. The full-energy peak efficiency,  $\varepsilon_p$ , and the effective solid angle will be calculated. It is important to mention that ANGLE software makes efficiency calculations only for coincidence-free gamma lines.

### 3.2. Neutron self-shielding and the spatial neutron flux distribution factors

In this step, the neutron self-shielding and the spatial neutron flux distribution factors [36, 40, 42–44] during irradiation in geological matrix were determined. The objective was to evaluate how significant were their contributions to the final elemental concentration results and which correction factor may be determined to correct the neutron flux gradient and self-shielding effects.

#### 3.2.1. Neutron self-shielding

Several programmes calculate the thermal neutron self-shielding factor ( $G_{th}$ ). To calculate this factor, it is necessary to know the sample composition and geometry. In this methodology development, the KayWin [39] and MATSSF software [45] were applied.

#### 3.2.2. Spatial neutron flux distribution factors

It is relevant to verify the axial and radial distributions of neutron fluxes in the vial. They can be evaluated experimentally during irradiation [40] and after by measuring the  $F_{c,Au}$ -factor, called the comparator factor, calculated based on neutron monitors irradiated together with the sample in sandwich form. This factor provides the trend of the axial neutron flux gradient, while radial gradient is negligible due to similar diameter of the sample and standard (Al-0.1% Au alloy).

Simplified equation of the  $k_0$ -method [21] for elemental concentration calculation for an analyte ( $a$ ), is below, Eq. (1):

$$\rho_a = \frac{A_{sp,a}}{F_{c,Au}} \cdot \frac{1}{k_{0,Au}(a)} \cdot \frac{1}{G_{th,a} \cdot f + G_{e,a} \cdot Q_{o,a}(\alpha)} \cdot \frac{1}{\varepsilon_{p,a}} \quad (1)$$

where the  $F_{c,Au}$ -factor, the comparator factor, Eq. (2), is:

$$F_{c,Au} = \frac{A_{sp,m} \cdot 10^{-6}}{k_{0,Au}(m)} \cdot \frac{1}{G_{th,m} \cdot f + G_{e,m} \cdot Q_{o,m}(\alpha)} \cdot \frac{1}{\varepsilon_{p,m}} \quad (2)$$

where  $A_{sp,m}$  and  $A_{sp,a}$  are the specific activities of monitor ( $m$ ) and analyte ( $a$ );  $k_{0,Au}(m)$  and  $k_{0,Au}(a)$  are  $k_0$ -factors of monitor Au (by definition  $\equiv 1$ ) and analyte;  $\varepsilon_{p,m}$  and  $\varepsilon_{p,a}$  are the full-energy peak detection efficiency of the monitor (Al-0.1%Au alloy in disc form) and radionuclide of analyte;  $f$  is thermal to epithermal neutron flux ratio;  $G_{th,m}$  and  $G_{th,a}$  are the correction factors for thermal neutron self-shielding;  $G_{e,m}$  and  $G_{e,a}$  are the correction factors for epithermal

neutron self-shielding;  $Q_{0,m}(\alpha)$  and  $Q_{0,a}(\alpha)$  are resonance integral ( $1/E^{1+\alpha}$ ) to 2200 m s<sup>-1</sup> cross-section ratio;  $\alpha$  is the epithermal flux distribution parameter.

Note that the  $F_{c,Au}$ -factor, as defined in Eq. (2), is proportional to the epithermal neutron flux density and directly indicates a gradient in epithermal flux density. In this study, the  $F_{c,Au}$ -factor was calculated by KayWin software based on several Al-0.1%Au monitors irradiated together with the samples in sandwich form.

### 3.3. Gamma-ray attenuation within the sample during counting

The  $k_0$ -method of NAA requires a precise technique to calculate full-energy peak detection efficiency ( $\epsilon_p$ ) of an HPGe detector for diversified samples and various counting geometries. The procedure provided by Moens et al. [46] presented a semi-empirical approach that has been introduced in KayWin software via option SOLCOI.

The basic principles are:

- a. A “reference” counting geometry is chosen to measure a set of calibrated point sources at a large distance, e.g., 15–20 cm;
- b. For a sample, the  $\epsilon_{p,geom}$  for particular gamma energy is expressed by employing the concept of the effective solid angle ( $\overline{\Omega}_{eff}$ ), with “ref” denoting the reference geometry and “geom” the actual one, Eq. (3):

$$\epsilon_{p,geom} = \epsilon_{p,ref} \cdot \frac{\overline{\Omega}_{geom}}{\overline{\Omega}_{ref}} \quad (3)$$

It is important to mention that by the definition of the effective solid angle, two factors are included: (i) the attenuation effects which gamma rays undergo outside an HPGe detector active zone,  $F_{att}$ -factor and (ii) the probability for an energy degradable gamma-ray interaction with the detector material,  $F_{eff}$ -factor. Both factors can be calculated analytically.

## 4. Experimental steps and results

In this study, the reference material IAEA-SOIL-7 (International Atomic Energy Agency (2000) [47] was analysed as a small cylindrical sample (SS), ~200 mg, and as a large cylindrical sample (LS), ~5 g. Neutron flux monitors and Al-0.1% Au disc, IRMM-530R (6 mm diameter-disc and 0.1 mm high) were used.

To carry out these experiments, according to Menezes and Jaćimović [16], the vials were prepared this way: (i) Vial 1, the large sample (LS): an aliquot of about 5 g of reference material IAEA-SOIL-7 was sealed in a polyethylene vial of 1.3 cm diameter and filled up

to 3.6 cm high. The first neutron flux monitor was placed below ampoule, the second inside the ampoule on the top of the sample, and the third outside the vial. Air space between the sample and top of vial was filled with cellulose paper; (ii) Vial 2: six polyethylene vials (9 mm in diameter and 5 mm high) filled with reference material IAEA-SOIL-7 were stacked with neutron flux monitors in sandwich form and inserted into a 5 cm high polyethylene vial; (iii) Vial 3, the small sample (SS): an aliquot of about 200 mg of reference material was sealed in a polyethylene vial (diameter of 9 mm and 5 mm high), stacked together with neutron flux monitors and inserted in a 5-cm-high vial. Air space between the sample and top of ampoule was filled with cellulose paper; (iv) Vial 4: the large sample (LS) was filled in with a soil aliquot, 3.6 cm high and 1.3 cm in diameter. After being prepared, each vial was inserted in the “rabbit”. **Figure 1** shows a scheme of the prepared vials.

#### 4.1. Detector efficiency over the volume source

In this step, the influence of distance sample-detector for small and large cylindrical samples based on gamma efficiency was verified. The LS, Vial 1, was measured at 2, 5, 10 and 20 cm sample-detector distances. The gamma efficiency values,  $\varepsilon_p$ , at sample-detector distances related to several gamma lines (non-coincidence gamma lines) and respective nuclides were given by KayWin software, [39] when calculating the elemental concentration of the large cylindrical sample. The efficiency values were also obtained by ANGLE software [41]. **Table 1** displays examples of the non-coincidence gamma energies for each nuclide determined and the respective ratio of each  $\varepsilon_p$  to  $\varepsilon_p$  of the reference distance sample-detector, 20 cm, for KayWin and ANGLE.

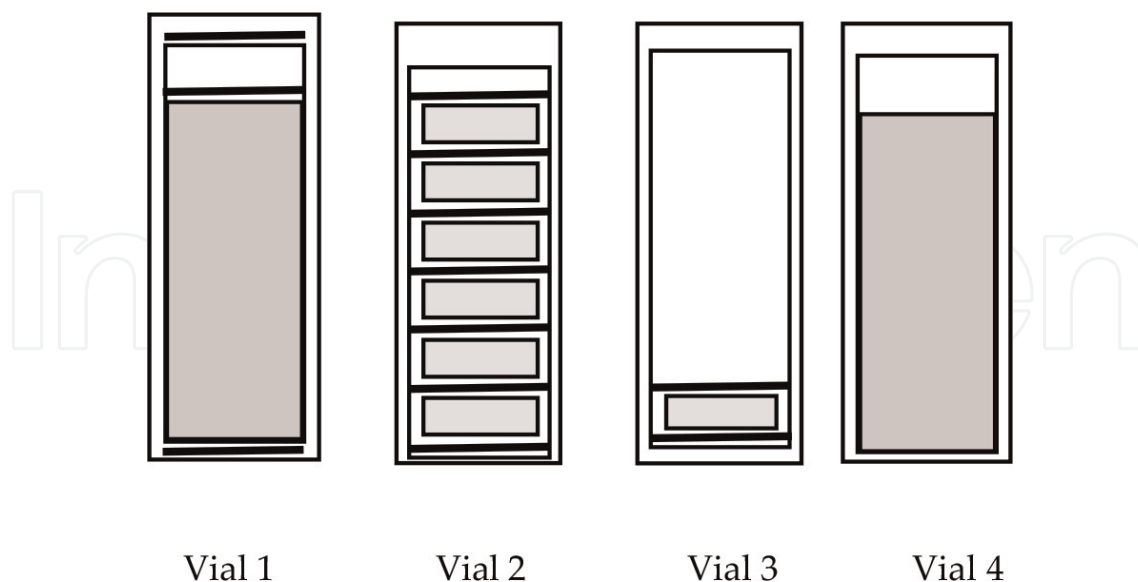


**Figure 1.** Vials prepared to carry out the experiments: Vial 1, large sample with reference material; Vial 2, with six small samples with reference material; Vial 3, with one small sample filled with reference material and Vial 4, with large sample filled with soil.



Nucl.	Non-coinc. gamma lines (keV)	Large sample ratio ( $\epsilon_p$ at specific distance (cm) to $\epsilon_p$ reference distance (cm) sample-detector)							
		KayWin				ANGLE			
		20/20	10/20	5/20	2/20	20/20	10/20	5/20	2/20
Sm-153	103.2	1.000	2.837	6.450	12.749	1.000	2.834	6.461	12.915
Ce-141	145.4	1.000	2.785	6.210	12.079	1.000	2.778	6.214	12.224
Sc-47	159.4	1.000	2.770	6.147	11.902	1.000	2.764	6.150	12.043
Au-199	208.2	1.000	2.734	5.987	11.455	1.000	2.727	5.989	11.589
Ru-97	215.7	1.000	2.730	5.970	11.405	1.000	2.724	5.974	11.546
Pa-233	300.1	1.000	2.699	5.832	11.024	1.000	2.693	5.838	11.163
Pa-233	311.9	1.000	2.697	5.821	10.993	1.000	2.690	5.827	11.132
Cr-51	320.1	1.000	2.695	5.814	10.972	1.000	2.688	5.819	11.111
Nd-147	531	1.000	2.667	5.693	10.637	1.000	2.660	5.695	10.763
As-76	559.2	1.000	2.665	5.682	10.607	1.000	2.657	5.685	10.733
Sb-122	564.2	1.000	2.664	5.680	10.602	1.000	2.657	5.683	10.728
Zn-65	1115.5	1.000	2.635	5.555	10.258	1.000	2.629	5.560	10.386
Fe-59	1291.6	1.000	2.630	5.532	10.194	1.000	2.623	5.538	10.323
K-42	1524.7	1.000	2.624	5.508	10.130	1.000	2.618	5.514	10.258
Sb-124	1691	1.000	2.621	5.495	10.094	1.000	2.615	5.502	10.223

**Table 1.** Non-coincidence gamma lines: ratio of gamma efficiency ( $\epsilon_p$ ) determined for a gamma line at a distance to gamma efficiency at reference distance sample-detector for the large sample, reference material IAEA-SOIL-7, Vial 1.

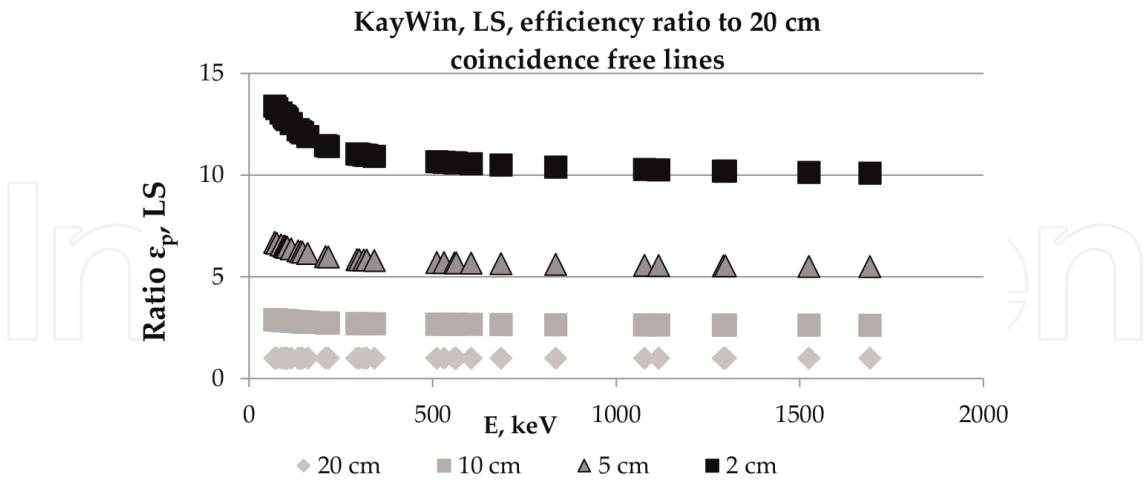


**Figure 2.** Gamma efficiency normalised to 20 cm obtained by KayWin software for the large cylindrical sample, LS, Vial 1 [16].

**Figures 2 and 3** display the gamma efficiency,  $\epsilon_p$ , calculated by gamma energy for distance sample-detector normalised to 20 cm for the HPGe detector D4. The figures show a good agreement—after 200 keV—between the ratio's efficiency,  $\epsilon_p$ , obtained by KayWin and ANGLE software at 2, 5, 10 and 20 cm and normalised to efficiency calculated at 20 cm.

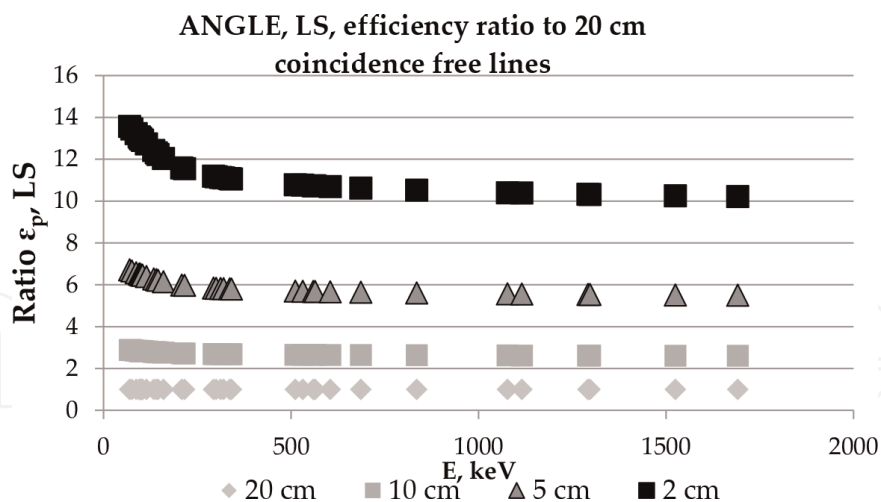


**Figure 3.** Gamma efficiency normalised to 20 cm obtained by ANGLE software for the large cylindrical sample, LS, Vial 1.

## 4.2. Neutron self-shielding and the spatial neutron flux distribution factors

### 4.2.1. Neutron self-shielding

In this methodology development, the KayWin [39] and MATSSF software [45] (specific to calculate the correction factor to thermal and epithermal neutron self-shieldings,  $G_{th}$  and  $G_e$ , respectively), were applied. A soil sample in cylindrical geometry, large sample, with diameter of 13 mm and 36 mm high was chosen to be studied. The composition,  $CaCO_3$  (80%) and  $SiO_2$  (20%), was assumed because these two components are typically major constitutions in soil matrices.

The KayWin calculated  $G_{th}$  equal to 0.997, while for the same configuration, the MATSSF obtained  $G_{th}$  equal to 0.998. There is a small difference from 1.0 for  $G_{th}$ , thermal neutron self-shielding. Due to this, no correction for thermal neutron self-shielding in the geological large sample was necessary. The  $G_e$  was considered negligible because of such experimental setup, i.e.,  $G_e = 1.0$ . The same approach has been taken for biological samples studied in this work (see Section 5), where  $G_{th} = G_e = 1.0$ .

### 4.2.2. Spatial neutron flux distribution factors

#### 4.2.2.1. Axial neutron flux gradient

To verify the axial and radial distributions of fast and thermal neutron fluxes in the same vial, Vial 4, experiments were carried out and are described in Jaćimović [48], and Menezes and partners [37], based on the experiment performed by Jaćimović and partners [40]. For these experiments, iron wires (99.9% Fe from Mallinckrodt, USA, 0.4 mm in diameter and 5 cm in length) were used.

During irradiation, the reactions were the following:

- $^{58}Fe(n, \gamma)^{59}Fe$ , 44.50 day half-life, gamma emissions of 1099.3 keV and 1291.6 keV from  $^{59}Fe$ ;
- $^{54}Fe(n, p)^{54}Mn$ , 312.2 day half-life, gamma emission of 834.8 keV from  $^{54}Mn$ .

The characterisation of neutron flux gradients (axial and radial) in the irradiation channels in the carousel facility was calculated. The calculation was based on the specific activities of  $^{59}\text{Fe}$  based on the mean value of the relative specific activities obtained for both gamma lines of  $^{59}\text{Fe}$  (thermal neutrons) and  $^{54}\text{Mn}$  (fast neutrons) applying the KayWin software. After decay time, about 2 weeks, the wires were cut into five 1-cm-pieces and submitted to gamma spectrometry on an HPGe detector D4 with 50% relative efficiency. The average specific activity of  $^{59}\text{Fe}$  was calculated based on the activity of 1099.3 and 1291.6 keV peaks and for  $^{54}\text{Mn}$ , on the peak of 834.8 keV.

One experiment was developed with one big vial filled with different materials, namely density, clay and air. The iron wires were placed in the vial: one in the centre and four near the wall of the polyethylene vial (3 cm in diameter and 5 cm high filled with clay) between the vial wall and the clay. **Figure 4**, position from the bottom (A = 0–1 cm) to top (E = 4–5 cm), related to thermal neutrons, shows the axial distributions for clay-air. The values of  $^{59}\text{Fe}$  were normalised to the average value of all the 1 cm Fe pieces. It can be observed that for thermal neutrons, the axial gradient in the geological sample is about 2%/cm. **Figure 5**, also related to thermal neutrons, shows the normalised radial distribution for clay-air. The figure points out that radial gradient for thermal neutrons in clay is about 2%/cm.

#### 4.2.2.2. $F_{c,Au}$ -factor

It was assumed that the  $F_{c,Au}$ -factor value is the correspondent to the average height of the sample. The  $F_{c,Au}$ -factors, calculated by KayWin based on Al-0.1%Au monitors in Vials 1 and 2, were used to verify the trend of axial gradient. Menezes and Jaćimović [16] pointed out that the  $F_{c,Au}$ -factors have a linear trend.

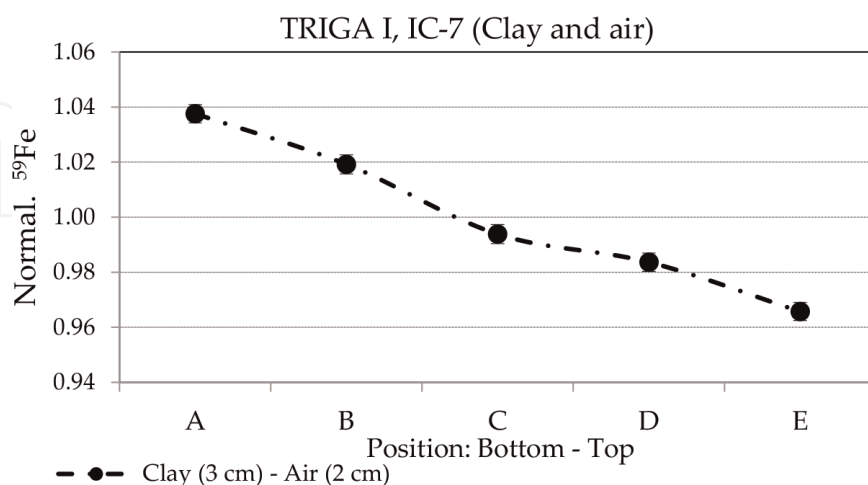


**Figure 4.** Axial gradient for thermal neutrons in clay-air in the IC-7 irradiation channel of the TRIGA reactor. The values are normalised related to  $^{59}\text{Fe}$  and error bars are calculated based on the average statistics counting of 1099.3 and 1291.6 keV from  $^{59}\text{Fe}$ , Vial 4 [37].

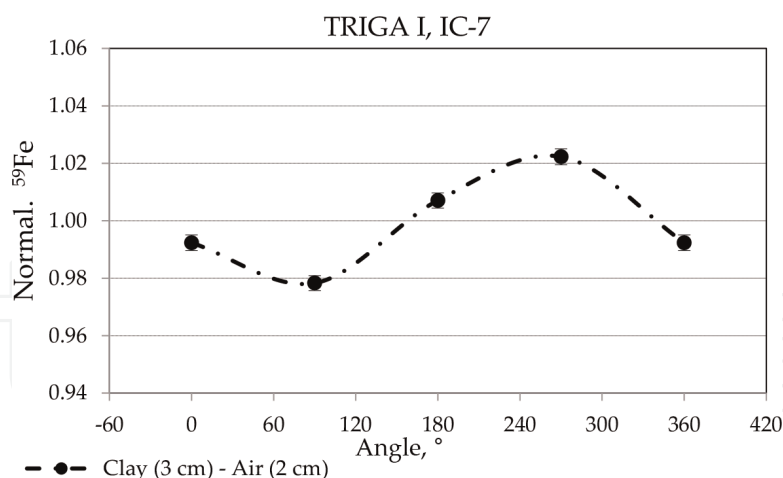


**Figure 5.** Radial gradient for thermal neutrons in clay-air in the IC-7 irradiation channel of the TRIGA reactor. The values are normalised related to <sup>59</sup>Fe and error bars are calculated based on the average statistics counting of 1099.3 and 1291.6 keV from <sup>59</sup>Fe, Vial 4 [37].

#### 4.3. Gamma-ray attenuation within the sample during counting

The programme KayWin makes several corrections as already mentioned in the subsection 3.3, Gamma-ray attenuation within the sample during counting, during elemental concentration calculations. As the values obtained for IAEA-SOIL-7 for small and large samples were according to recommended values, according to next subsection 5 (Comparison between small and large samples' elemental concentration results), it was not necessary to develop more tests and apply correction factors.

### 5. Comparison between small and large samples' elemental concentration results

KayWin software calculated the efficiencies of the large sample accordingly, and the calculated  $F_{c,Au}$ -factors for the large sample obtained for Al-0.1% Au monitors were described by a linear equation. Then, it was decided to verify the experimental mass fractions for the small (Vial 3) and the large sample (Vial 1). The samples were measured at 2, 5, 10 and 20 cm at detector D4 (50% relative efficiency), and the elemental concentrations were calculated for each distance and for several distances, called RP, a routine procedure of analysis for customers, i.e., suitable distance sample-detector depending on the activity/dead-time. The experimental results and recommended values for reference material IAEA-SOIL-7 calculated by KayWin are shown in Menezes and Jaćimović [16].

**Table 2** shows the normalised values of small and large samples to IAEA-SOIL-7 recommended data. It is possible to observe that majority of results are within 95% of confidence interval for assigned values. For the small sample, 88% of the results presented deviations from the recommended values lower than 10%, while for cylindrical samples, the deviations were 74%. For both samples measured at 10 cm, they presented 12% of deviations, and it was the best

El.	Recommended values (mg kg <sup>-1</sup> )	Normalised values on IAEA-SOIL-7 recommended data (date of issue: 2000)									
		Ratio result obtained at specific distance (cm)/recommended value									
		Small sample (~200 mg)					Large sample (~5 g)				
		2	5	10	20	RP	2	5	10	20	RP
As	13.4 ± 0.85	1.11	1.05	1.07	1.04	1.09	1.17	1.15	1.15	1.12	1.15
Ce	61 ± 6.50	1.00	0.97	0.95	0.95	1.00	1.04	0.99	0.98	0.97	1.01
Co	8.9 ± 0.85	1.05	1.03	1.02	1.07	1.05	1.06	1.04	1.04	1.02	1.06
Cr	60 ± 12.5	1.22	1.18	1.16	1.15	1.15	1.30	1.25	1.26	1.22	1.30
Cs	5.4 ± 0.75	1.05	1.05	1.05	1.05	1.05	1.11	1.09	1.09	1.08	1.10
Eu	1.0 ± 0.2	1.02	1.07	1.10	0.85	0.95	1.12	1.17	1.08	1.10	1.12
Hf	5.1 ± 0.35	1.04	1.02	1.01	1.01	1.04	1.05	1.04	1.04	1.01	1.03
La	28 ± 1	1.06	1.01	1.02	1.01	1.04	1.07	1.05	1.04	1.03	1.04
Nd	30 ± 6	0.87	0.94	0.92	0.95	0.88	0.98	1.10	1.02	1.09	1.08
Rb	51 ± 4.5	1.04	0.99	0.97	0.97	1.04	1.09	1.03	1.03	1.04	1.04
Sb	1.7 ± 0.2	1.08	1.06	1.08	1.07	1.08	1.07	1.03	1.02	1.03	1.03
Sc	8.3 ± 1.05	1.12	1.10	1.08	1.08	1.12	1.13	1.11	1.10	1.09	1.11
Sm	5.1 ± 0.35	0.96	0.98	0.93	0.92	0.96	1.03	1.01	0.98	0.96	1.01
Ta	0.8 ± 0.2	0.91	0.94	0.93	0.93	0.91	0.95	0.98	0.98	0.97	0.95
Tb	0.6 ± 0.2	1.10	1.13	1.10	1.10	1.10	1.22	1.19	1.14	1.15	1.21
Th	8.2 ± 1.1	1.02	1.01	0.98	0.97	1.02	1.08	1.06	1.05	1.03	1.08
U	2.6 ± 0.55	0.90	0.85	0.87	0.85	0.85	0.99	0.90	0.91	0.89	0.90
Yb	2.4 ± 0.35	1.00	0.98	0.95	0.94	1.00	1.06	0.99	0.99	0.98	0.99
Zr	185 ± 10.5	1.12	1.11	1.13	1.12	1.13	1.29	1.14	0.94	1.06	1.30

El., element; RP, calculations carried out according to the usual procedure to the customers.

**Table 2.** Normalised values of small (Vial 3) and large samples (Vial 1) obtained at specific distance to IAEA-SOIL-7 on recommended data [16].

performance. Kennedy and St-Pierre [49] in their work observed a similar conclusion, where 10 cm distance sample-detector shows the best performance. The authors used an HPGe detector with 29% relative efficiency. Same conclusion can be explained due to the same method used for the absolute calibration procedure of an HPGe detector. Nevertheless, results presented in **Table 2** for IAEA-SOIL-7 show relatively small differences between measurement distance sample-detector. So, it is possible to conclude that the impact from different measurement positions (or ratio between measurement and reference position) contributed relatively small systematic error to the final result.

The analytical performance of the experiments and the agreement of element contents with recommended values, the assigned values for IAEA-SOIL-7, i.e., the data given in the Certificate of analysis in 2000 [47] were evaluated by the statistical test called  $E_n$ -score [50]. This score

takes into account the expanded uncertainty of both values with a coverage factor  $k = 2$  (95% confidence interval). At CDTN, the uncertainty of the  $k_0$ -NAA established is considered as 3.5% with a coverage factor  $k = 1$ .  $E_n$ -score is calculated as follows:

$$E_n = \frac{X_{lab} - X_{ref}}{\sqrt{U_{lab}^2 + U_{ref}^2}} \quad (4)$$

where  $X_{lab}$  and  $X_{ref}$  are laboratory and reference (assigned value) values, respectively;  $U_{lab}$  and  $U_{ref}$  are expanded uncertainties with a coverage factor  $k = 2$  of laboratory and reference values, respectively. The criterion  $|E_n| \leq 1$  was applied to compare the results of the two geometries with reference data, meaning that the evaluation of the performance of the method was satisfactory, producing values with a level of confidence of about 95% and if  $|E_n| > 1$ , the performance was unsatisfactory. **Table 3** displays the results for this test.

Element	Recommended values (mg kg <sup>-1</sup> )	Experimental values			
		Small sample		Large sample	
		(mg kg <sup>-1</sup> )	$E_n$	(mg kg <sup>-1</sup> )	$E_n$
As	13.4 ± 0.85	14.2 ± 0.5	0.59	14.2 ± 0.5	0.56
Ce	61 ± 6.5	60.8 ± 2.1	0.03	59.9 ± 2.1	0.13
Co	8.9 ± 0.85	9.33 ± 0.33	0.40	9.17 ± 0.32	0.25
Cr	60 ± 12.5	68.9 ± 4.0	0.60	63.6 ± 2.6	0.27
Cs	5.4 ± 0.75	5.69 ± 0.20	0.35	5.83 ± 0.21	0.50
Eu	1.0 ± 0.2	0.95 ± 0.03	0.24	1.12 ± 0.16	0.33
Hf	5.1 ± 0.35	5.33 ± 0.20	0.43	5.34 ± 0.19	0.46
La	28 ± 1	29 ± 1	0.44	29 ± 1	0.42
Nd	30 ± 6	26.3 ± 1.2	0.57	27.9 ± 1.3	0.32
Rb	51 ± 4.5	53.0 ± 2.4	0.31	51.8 ± 2.5	0.12
Sb	1.7 ± 0.2	1.83 ± 0.07	0.54	1.73 ± 0.06	0.14
Sc	8.3 ± 1.05	9.29 ± 0.33	0.80	9.09 ± 0.32	0.65
Sm	5.1 ± 0.35	4.87 ± 0.19	0.44	5.22 ± 0.18	0.24
Ta	0.8 ± 0.2	0.73 ± 0.03	0.33	0.78 ± 0.03	0.11
Tb	0.6 ± 0.2	0.66 ± 0.02	0.30	0.69 ± 0.02	0.45
Th	8.2 ± 1.1	8.35 ± 0.29	0.12	8.61 ± 0.30	0.32
U	2.6 ± 0.55	2.21 ± 0.13	0.64	2.55 ± 0.10	0.09
Yb	2.4 ± 0.35	2.39 ± 0.09	0.03	2.37 ± 0.09	0.08

Uncertainties of recommended values are given at a confidence interval of 95% ( $k = 2$ ), while experimental values are given as combined standard uncertainty.

**Table 3.** Experimental results and recommended values for IAEA-SOIL-7 analysed as small (Vial 3) and large samples (Vial 1) [37].



6. Some applications

In order to confirm the applicability and its ability to produce good results, several reference materials were analysed as small and large samples. **Tables 4–6** show the results of certified

BCR-320R, channel sediment					
Element	Certified values, $k = 2$  (mg kg <sup>-1</sup> )	Experimental results, $k = 1$			
		Small sample, $n = 3$ , (~0.150 g)		Large samples, $n = 3$ , (~1 g)	
		(mg kg <sup>-1</sup> )	$E_n$	(mg kg <sup>-1</sup> )	$E_n$
As	21.7 ± 2.0	21.2 ± 0.7	0.19	21.5 ± 0.9	0.08
Co	9.7 ± 0.6	9.3 ± 0.3	0.48	9.2 ± 0.3	0.54
Cr	59 ± 4	58 ± 2	0.19	57 ± 3	0.39
Fe	25,700 ± 1300	24,180 ± 851	0.71	24,100 ± 867	0.74
Sc	5.2 ± 0.4	5.0 ± 0.2	0.41	5.0 ± 0.2	0.37
Th	5.3 ± 0.4	5.0 ± 0.2	0.51	4.9 ± 0.2	0.68
U	1.56 ± 0.20	1.5 ± 0.1	0.29	1.4 ± 0.1	0.49
Zn	319 ± 20	304 ± 11	0.48	310 ± 11	0.28

$n$ , number of replicates.

**Table 4.** Mass fractions obtained for certified reference material BCR-320R, *Channel Sediment*, analysed as small and large samples [51].

Element	NIST SRM 1572, citrus leaves				
	Certified values, $k = 2$  (mg kg <sup>-1</sup> )	Experimental results, $k = 1$			
		Small sample (0.2124 g)		Large sample (2.4758 g)	
		(mg kg <sup>-1</sup> )	$E_n$	(mg kg <sup>-1</sup> )	$E_n$
As	3.1 ± 0.3	3.5 ± 0.1	0.91	2.8 ± 0.1	0.78
Ba	21 ± 3	21 ± 2	0.09	18 ± 1	0.97
Ca	31,500 ± 1000	34,780 ± 1554	1.00	29,150 ± 1098	0.97
Cr	0.8 ± 0.2	0.8 ± 0.1	0.12	0.81 ± 0.05	0.05
Fe	90 ± 10	108 ± 8	0.95	98 ± 4	0.58
Hg	0.08 ± 0.02	< 0.2	—	0.09 ± 0.01	0.42
K	18,200 ± 600	20,570 ± 1200	0.96	17,360 ± 684	0.56
Na	160 ± 20	185 ± 7	1.00	165 ± 6	0.22
Rb	4.84 ± 0.06	5.3 ± 0.5	0.54	4.5 ± 0.2	0.90
Sr	100 ± 2	111 ± 8	0.73	94 ± 4	0.61

**Table 5.** Mass fractions obtained for certified reference material NIST SRM 1572, *Citrus Leaves*, analysed as small and large samples [52].

Element	NIES no 7, <i>tea leaves</i>				
	Certified values, $k = 2$	Experimental results, $k = 1$			
		Small sample (0.3024 g)		Large sample (3.5517 g)	
		(mg kg <sup>-1</sup> )	$ E_n $	(mg kg <sup>-1</sup> )	$ E_n $
Br	2.5 ± 0.1	2.8 ± 0.2	0.77	2.4 ± 0.1	0.56
Ca	3200 ± 120	3607 ± 266	0.75	2794 ± 200	0.97
Fe	98 ± 7	114 ± 9	0.84	98 ± 5	0.01
K	18,600 ± 700	20,240 ± 800	0.94	18,200 ± 687	0.26
La	0.068 ± 0.002	0.080 ± 0.006	1.00	0.064 ± 0.003	0.58
Na	15.5 ± 1.5	18 ± 1	0.97	18 ± 1	1.00
Rb	6.59 ± 0.01	6.7 ± 0.3	0.14	5.8 ± 0.5	0.93

**Table 6.** Mass fractions obtained for reference material NIES no 7, *tea leaves*, analysed as small and large samples [52].

El.	Oatmeal powder			Chia powder		
	Small sample (0.2040 g)	Large sample (0.6085 g)	Large sample (2.5396 g)	Small sample (0.2415 g)	Large sample (0.5703 g)	Large sample (3.4228 g)
	(mg kg <sup>-1</sup> )	(mg kg <sup>-1</sup> )	(mg kg <sup>-1</sup> )	(mg kg <sup>-1</sup> )	(mg kg <sup>-1</sup> )	(mg kg <sup>-1</sup> )
Ba	<10	8 ± 1	8 ± 1	45 ± 2	45 ± 2	45 ± 2
Br	1.88 ± 0.07	1.81 ± 0.06	1.79 ± 0.06	8.7 ± 0.3	8.8 ± 0.3	8.0 ± 0.3
Ca	<690	643 ± 127	553 ± 87	7081 ± 504	7281 ± 462	6918 ± 572
Co	0.024 ± 0.007	0.029 ± 0.002	0.030 ± 0.003	0.35 ± 0.01	0.35 ± 0.02	0.37 ± 0.02
Cs	0.087 ± 0.005	0.092 ± 0.004	0.086 ± 0.004	0.044 ± 0.004	0.044 ± 0.003	0.044 ± 0.003
Fe	56 ± 7	60 ± 3	56 ± 3	118 ± 6	97 ± 5	109 ± 5
K	4134 ± 146	4175 ± 148	3972 ± 140	8531 ± 300	8618 ± 304	8213 ± 291
La	<0.01	<0.01	<0.01	0.069 ± 0.006	0.062 ± 0.004	0.073 ± 0.003
Mo	0.5 ± 0.1	<0.6	0.6 ± 0.1	<0.4	<0.4	<0.4
Na	10 ± 1	10.6 ± 0.4	10.9 ± 0.4	7.3 ± 0.2	7.2 ± 0.3	8.8 ± 0.4
Rb	9.0 ± 0.4	8.7 ± 0.4	8.3 ± 0.3	11.8 ± 0.5	11.8 ± 0.5	11.9 ± 0.5
Sc*	2.9 ± 0.4	1.8 ± 0.3	1.6 ± 0.3	<0.02	<0.02	<0.02
Sm	<0.004	<0.004	<0.004	<0.008	0.008 ± 0.002	0.010 ± 0.001
Sr	<10	<10	<10	46 ± 3	47 ± 3	45 ± 2
Ta	<0.01	<0.005	0.018 ± 0.004	<0.03	<0.03	<0.03
Zn	<32	<32	<32	61 ± 2	61 ± 2	51 ± 2

El., element; experimental values are given as combined standard uncertainty.

\* µg kg<sup>-1</sup>.

**Table 7.** Mass fractions obtained for oatmeal powder and chia powder analysed in three sizes of samples: one small and two large samples [53].

Element    Soil sample					
	Small sample (0.1133 g) (mg kg <sup>-1</sup> )	Large sample (0.6313 g) (mg kg <sup>-1</sup> )	Element	Small sample (0.1133 g) (mg kg <sup>-1</sup> )	Large sample (0.6313 g) (mg kg <sup>-1</sup> )
Fe	23,070 ± 952	22,100 ± 1235	Ta	2.31 ± 0.09	2.26 ± 0.12
Ga	37.2 ± 1.3	33.9 ± 1.2	Tb	0.503 ± 0.032	0.515 ± 0.019
Hf	32.8 ± 1.5	30.4 ± 2.0	Th	31.0 ± 1.3	29.9 ± 1.5
K	347 ± 30	367 ± 25	U	3.71 ± 0.14	3.49 ± 0.15
La	70.3 ± 2.7	70.0 ± 2.5	W	13.4 ± 0.5	13.7 ± 0.5
Sb	0.471 ± 0.046	0.430 ± 0.038	Yb	5.61 ± 0.36	5.21 ± 0.15
Sc	10.4 ± 0.4	9.7 ± 0.5	Zn	15.2 ± 1.9	16.0 ± 2.1

Experimental values are given as combined standard uncertainty.

**Table 8.** Mass fractions obtained for soil, analysed as small and large samples.

reference materials, BCR-320R, *Channel Sediment*, NIST SRM 1572, *Citrus Leaves*, and reference material, NIES no 7, *Tea Leaves*, respectively. **Tables 7** and **8** show examples of samples analysed at the Laboratory for Neutron Activation Analysis, as small and large samples.

7. Conclusions

The Laboratory for Neutron Activation Analysis at CDTN, Brazil, needs to be prepared to meet customer analysis requirements. In order to answer this requirement, it was necessary to establish a methodology to analyse large samples, from 0.5 to 5 g sample, applying the *k<sub>0</sub>*-standardised method keeping the current infrastructure for irradiation and gamma measurements. Another objective was to overcome technical limitations while analysing samples smaller than 0.5 g, as, for instance, inhomogeneity of the sample and lower thermal neutron flux of the reactor.

To carry out the establishment, it was necessary to calculate several relevant parameters that would point out the feasibility to analyse large samples: detector efficiency over the volume source, neutron self-shielding during neutron irradiation and gamma-ray attenuation within the sample during counting.

The results [16, 36, 37] pointed out that all parameters may be negligible for the large sample. At least, within the uncertainty range, once the elemental concentration results are in good agreement with the recommended values of the reference material IAEA-SOIL-7. All results obtained during the development using the reference material were evaluated by the statistical test, *E<sub>n</sub>-score*, which pointed out that the *k<sub>0</sub>*-method applied using KayWin software presented an overall satisfactory performance. Few exceptions are already being investigated using other reference materials. It means that the KayWin software proved to be a robust programme to calculate the elemental concentration of large samples producing reliable results.

It is important to note that once the methodology is established, the following benefits may be obtained: reaching lower limits of detection; enabling compliance, for example, in environmental legislation in determining the concentration of metals in soil; analyses of more representative aliquots, especially in the case of non-homogeneous samples, as industrial waste; optimization of the cost and time of analysis, because instead of analysing several small samples they could be replaced by a large sample; analyses of whole parts when removing the aliquots are not possible. This study is still going on in order to confirm the benefits that have been already mentioned.

This investigation has confirmed that any other laboratory applying  $k_0$ -instrumental neutron activation analysis ( $k_0$ -INAA) is able to establish this methodology without having to modify its facilities, since the neutron self-shielding, gamma attenuation and detector efficiency over the volume sample are established.

## Acknowledgements

This work was partially supported by the International Atomic Energy Agency under grant BRA-14798, by the Brazilian Foundation for Research Support of Minas Gerais, FAPEMIG, under grant APQ-01259-09, and by financial support from the Slovenian Research Agency (ARRS) through programme P1-0143. Thanks to Brazilian National Council for Scientific and Technological Development, CNPq, and to Coordination for the Improvement of Higher Education Personnel, CAPES. Thanks to the TRIGA MARK I IPR-R1 reactor staff for making the use of the reactor for the experiments possible. Last but not least thanks to Dr Tibor G. Kocsor (*Journal of Radioanalytical and Nuclear Chemistry*) for allowing the use of tables and figures previously published.

## Author details

Maria Ângela de B.C. Menezes<sup>1\*</sup> and Radojko Jaćimović<sup>2</sup>

\*Address all correspondence to: [menezes@cdtn.br](mailto:menezes@cdtn.br)

1 Nuclear Technology Development Centre, Brazilian Commission for Nuclear Energy, CDTN/CNEN, Belo Horizonte, Minas Gerais, Brazil

2 Jožef Stefan Institute, Ljubljana, Slovenia

## References

- [1] Hamidatou L, Slamene H, Akhal T, Zouranen B. Concepts, Instrumentation and techniques of neutron activation analysis. In: Kharfi F, editor. *Imaging and Radioanalytical Techniques in Interdisciplinary Research*. IntechOpen. DOI: 10.5772/53686. Available

from: <https://www.intechopen.com/books/imaging-and-radioanalytical-techniques-in-interdisciplinary-research-fundamentals-and-cutting-edge-applications/concepts-instrumentation-and-techniques-of-neutron-activation-analysis>

- [2] De Soete D, Gijbels R, Hoste J. Neutron activation analysis. A Series of Monographs on Analytical Chemistry and Its Applications Chemical Analysis. Vol. 34. Wiley-Interscience; 1972. p. 836
- [3] Bode P. Opportunities for innovation in neutron activation analysis. Journal of Radioanalytical and Nuclear Chemistry. 2012;**291**:275-280
- [4] Greenberg RR, Bode P, Fernandes EAN. Neutron activation analysis: A primary method of measurement. Spectrochimica Acta, Part B: Atomic Spectroscopy. 2011;**66**:193-241
- [5] De Corte F, Simonits A, De Wispelaere A, Hoste J. Accuracy and applicability of the  $k_0$ -standardization method. Journal of Radioanalytical and Nuclear Chemistry. 1987;**113**: 145-161
- [6] Jaćimović R, Smodiš B, Bučar T, Stegnar P.  $k_0$ -NAA quality assessment by analysis of different certified reference materials using the KAYZERO/SOLCOI software. Journal of Radioanalytical and Nuclear Chemistry. 2003;**257**:659-663
- [7] Leal AS, Menezes MABC, Jaćimović R, Sepe FP, Gomes TCB. Investigation of the quality of the drug Enalapril commercialized by pharmacies of manipulation in Belo Horizonte, Brazil. Journal of Radioanalytical and Nuclear Chemistry. 2014;**300**:645-651
- [8] Menezes MABC, Sabino CVS, Franco MB, Kastner GF, Rossi Montoya EH.  $k_0$ -Instrumental Neutron Activation analysis establishment at CDTN, Brazil: A successful story. Journal of Radioanalytical and Nuclear Chemistry. 2003;**257**:627-632
- [9] Menezes MABC, Jaćimović R. Optimised  $k_0$ -instrumental neutron activation method using the TRIGA MARK I IPR-R1 reactor at CDTN/CNEN, Belo Horizonte, Brazil. Nuclear Instruments and Methods in Physics Research A. 2006;**564**:707-715
- [10] Menezes MABC, Maia ECP, Albinati CCB, Sabino CVS, Batista JR. How suitable are scalp hair and toenail as biomonitors? Journal of Radioanalytical and Nuclear Chemistry. 2004;**259**:81-86
- [11] Menezes MABC, Maia ECP, Albinati CCB. Instrumental neutron activation analysis as an analytical tool on supporting the establishment of guidelines and data basis for worker's health awareness program. Revista Brasileira de Pesquisa e Desenvolvimento. 2002;**4**:1110-1117
- [12] Menezes MABC, Palmieri HEL, Leonel LV, Nalini HA Jr, Jaćimović R. Iron Quadrangle, Brazil: Elemental concentration determined by  $k_0$ -instrumental neutron activation analysis Part I: soil samples. Journal of Radioanalytical and Nuclear Chemistry. 2006;**270**:111-116
- [13] Menezes MABC, Palmieri HEL, Leonel LV, Nalini HA Jr, Jaćimović R. Elemental concentration determined by  $k_0$ -instrumental neutron activation analysis Part II: kale samples. Journal of Radioanalytical and Nuclear Chemistry. 2006;**270**:117-121

- [14] Menezes MABC, Pelaes ACO, Salles PMB, Silva WF, Moura RR, Moura IFS, Jaćimović R. Neutron activation technique: A reliable tool to determine the mineral composition in agro-industrial products. *Radiation and Applications*. 2017;**2**:124-128
- [15] Menezes MABC, Sabino CVS, Franco MB, Maia ECP, Albinati CCB. Assessment of Workers' Contamination caused by air pollution exposure in industry using biomonitors. *Journal of Atmospheric Chemistry*. 2004;**49**:403-414
- [16] Menezes MABC, Jaćimović R. Implementation of a methodology to analyse cylindrical 5-g sample by neutron activation technique,  $k_0$  method, at CDTN/CNEN, Belo Horizonte, Brazil. *Journal of Radioanalytical and Nuclear Chemistry*. 2014;**300**:523-531
- [17] Salles PMB, Menezes MABC, Sathler MM, Moura RR, Campos TPR. Inorganic elements in sugar samples consumed in several countries. *Journal of Radioanalytical and Nuclear Chemistry*. 2015;**306**:1-9
- [18] Salles PMB, Menezes MABC, Sathler MM, Moura RR, Campos TPR. Elemental composition of dietary supplements most consumed in Belo Horizonte, Brazil, analysed by  $k_0$ -INAA. *Journal of Radioanalytical and Nuclear Chemistry*. 2017;**308**:1-5
- [19] Silveira JN, Menezes MABC, Lara PCP, Beininger MA, Silva JBB. Determination of Al, Ca, Cl, Cr, K, Mg, Sb and Ti in industrialized and formulated antihypertensive drugs using Neutron Activation Analysis. *Journal of Pharmacy and Biological Sciences*. 2015;**10**:40-45
- [20] Viana CO, Menezes MABC, Maia ECP. Epiphytic lichens on air biomonitoring in Belo Horizonte City, Brazil: A preliminary assessment. *International Journal of Environment and Health*. 2011;**5**:324-336
- [21] De Corte F. The  $k_0$ -Standardisation Method: A Move to the Optimisation of Neutron Activation Analysis [thesis]. Ryksuniversiteit Ghent, Faculteit Van de Wetenschappen; 1987
- [22] De Corte F, Simonits A. Recommended nuclear data for use in the  $k_0$  standardization of neutron activation analysis. *Atomic Data and Nuclear Data Tables*. 2003;**85**:47-67
- [23] Jaćimović R, De Corte F, Kennedy G, Vermaercke P, Revay Z. The 2012 recommended  $k_0$  database. *Journal of Radioanalytical and Nuclear Chemistry*. 2014;**300**:589-592
- [24]  $k_0$ -database 2015 [Internet]. 2015. Available from: [http://www.kayzero.com/k0naa/k0naaorg/Nuclear\\_Data\\_SC/Entries/2016/1/11\\_New\\_k0-data\\_Library\\_2015.html](http://www.kayzero.com/k0naa/k0naaorg/Nuclear_Data_SC/Entries/2016/1/11_New_k0-data_Library_2015.html) [Accessed: 25-10-2018]
- [25] Bode P, Overwater RMW, De Goeij JJM. Large-sample neutron activation analysis: Present status and prospects. *Journal of Radioanalytical and Nuclear Chemistry*. 1997;**216**:5-11
- [26] Gwozdz R. Instrumental neutron activation analysis of samples with volumes from 2 to 350 ml. *Journal of Radioanalytical and Nuclear Chemistry*. 2007;**271**:751-759
- [27] Tzika F, Stamatelatos IE, Kalef-Ezra J. Neutron activation analysis of large samples: The influence of inhomogeneity. *Journal of Radioanalytical and Nuclear Chemistry*. 2007;**271**: 233-240
- [28] Blaauw M, Lakmaker O, Van Aller P. The accuracy of instrumental neutron activation analysis of kilogram-size inhomogeneous samples. *Analytical Chemistry*. 1997;**69**:2247-2250



- [29] Shakir NS, Jarvis RE. Correction factors required for quantitative large volume INAA. *Journal of Radioanalytical and Nuclear Chemistry*. 2001;**248**:61-68
- [30] Lin X, Henkelmann R. Instrumental neutron activation analysis of large samples: A pilot experiment. *Journal of Radioanalytical and Nuclear Chemistry*. 2002;**251**:197-204
- [31] Overwater RMW. The Physics of Big Sample Instrumental Neutron Activation Analysis [thesis]. Delft: Delft University of technology; 1994
- [32] Stamatelatos IE, Tzika F. Large sample neutron activation analysis: A challenge in cultural heritage studies. *Annali di Chimica*. 2007;**97**:505-512
- [33] Lindstrom RM, Fleming RF. Neutron self-shielding factors for simple geometries, Revisited. *Chemist-Analyst*. 2008;**53**:855-859
- [34] Musa Y, Ahmed YA, Yamusa YA, Ewa IOB. Determination of radial and axial neutron flux distribution in irradiation channel of NIRR-1 using foil activation technique. *Annals of Nuclear Energy*. 2012;**50**:50-55
- [35] Tzika F, Stamatelatos IE, Kalef-Ezra J, Bode P. Large sample neutron activation analysis: Correction for neutron and gamma attenuation. *Nukleonika*. 2004;**49**:115-121
- [36] Menezes MABC, Jaćimović R, Ribeiro L. Contribution of analytical nuclear techniques in the reconstruction of the Brazilian prehistory analysing archaeological ceramics of Tupiguarani tradition. In: International Atomic Energy Agency, editor. *Advances in Neutron Activation Analysis of Large Objects with Emphasis on Archaeological Examples*. Research Project. IAEA-TECDOC-1838; 2018. pp. 4-21
- [37] Menezes MABC, Jaćimović R, Pereira C. Spatial distribution of neutron flux in geological larger sample analysis at CDTN/CNEN, Brazil. *Journal of Radioanalytical and Nuclear Chemistry*. 2015;**306**:611-616
- [38] HyperLab Gamma Spectroscopy Software, HyperLabs, Software [Internet]. 2009. Available from: <http://hlabsoft.com/> [Accessed: 09-06-2013]
- [39] Van Sluijs R. Kayzero for Windows User's Manual, for reactor neutron activation analysis (NAA) using the  $k_0$  standardisation method, V. 2. Software developed by DSM Research, Geleen (NL) for NAA based on the  $k_0$  standardization method developed at the INW-RUG, Gent (B) and the AEKI, Budapest (H).  *$k_0$ -Ware*, Heerlen, The Netherlands, 2011. Available: <http://www.kayzero.com/KfW%20Manual%20V1.pdf> [Accessed: 2013-06-12]
- [40] Jaćimović R, Stibilj V, Benedik L, Smodiš B. Characterization of the neutron flux gradients in typical irradiation channels of a TRIGA Mark II reactor. *Journal of Radioanalytical and Nuclear Chemistry*. 2003;**257**:545-549
- [41] Jovanović S, Dlabáč A, Mihaljević N, Vukotić P. ANGLE: A PC-code for semiconductor detector efficiency calculations. *Journal of Radioanalytical and Nuclear Chemistry*. 1997;**218**:13-20
- [42] Matsushita R, Koyama M, Yamada S, Kobayashi M, Moriyama H. Neutron flux gradients and spectrum changes in the irradiation capsule for reactor neutron activation analysis. *Journal of Radioanalytical and Nuclear Chemistry*. 1997;**216**:95-99

- [43] Arbocco FF, Vermaercke P, Sneyers L, Strijckmans K. Experimental validation of some thermal neutron self-shielding calculation methods for cylindrical samples in INAA. *Journal of Radioanalytical and Nuclear Chemistry*. 2011;**291**:529-534. DOI: 10.1007/s10967-011-1211-y
- [44] Chilian C, St-Pierre J, Kennedy G. Dependence of thermal and epithermal neutron self-shielding on sample size and irradiation site. *Nuclear Instruments and Methods in Physics Research Section A: Accelerators, Spectrometers, Detectors and Associated Equipment*. 2006;**564**:629-635
- [45] Trkov A, Žerovnik G, Snoj L, Ravnik M. On the self-shielding factors in neutron activation analysis. *Nuclear Instruments and Methods in Physics Research A*. 2009;**610**:553-565
- [46] Moens L, De Donder J, Xi-lei L, De Corte F, De Wispelaere A, Simonits A, Hoste J. Calculation of the absolute peak efficiency of gamma-ray detectors for different counting geometries. *Nuclear Instruments and Methods in Physics Research*. 1981;**187**:451-472
- [47] Analytical Quality Control Services (AQCS) Agency's Laboratories. International Atomic Energy Agency Certified reference material IAEA-SOIL-7. IAEA, Vienna, 2000
- [48] Jaćimović R. Activities Developed During the Period of the Fellowship BEV, Process CNPq 170058/2011-5 and Institutional Process 551042/2011-7 [report]. Belo Horizonte: Nuclear Technology Development Centre (Centro de Desenvolvimento da Tecnologia Nuclear, CDTN); 2011
- [49] Kennedy G, St-Pierre J. Is the  $k_0$  method accurate for elements with high  $Q_0$  values? *Journal of Radioanalytical and Nuclear Chemistry*. 2003;**257**:475-480
- [50] ISO 13528. Statistical Methods for Use in Proficiency Testing by Interlaboratory Comparisons. 2nd ed. Geneva (CH): International Organization for Standardization; 2015
- [51] Pelaes AC. Avaliação da incerteza de medição da composição de amostras geológicas analisadas por meio do método  $k_0$  de ativação neutrônica (Evaluation of the uncertainty of the measurement of geological samples analysed by neutron activation analysis,  $k_0$ -method). [dissertation], Belo Horizonte: Postgraduate Program in Radiation, Minerals and Materials Science and Technology, CDTN; 2018
- [52] Sathler MM, Salles PMB, Oliveira HS, Menezes MABC. Amostras grandes analisadas por ativação neutrônica, método  $k_0$  (Large samples analysed by neutron activation analysis,  $k_0$  method). In: *Proceedings of the Quarta Semana de Engenharia Nuclear e Ciências das Radiações (Forth Week of Nuclear Engineering and Sciences of Radiation) (IV SENCIR 2018)*; Belo Horizonte, 6-8 November 2018. Belo Horizonte: PPCTN, UFMG; 2018. pp. 107-112
- [53] Sathler MM. Avaliação da composição elementar de alimentos integrais e refinados por meio do método  $k_0$  de ativação neutrônica aplicado a amostras grandes (Evaluation of the elemental composition of integral and refined foods by  $k_0$ -neutron activation method applied to large samples). [dissertation], Belo Horizonte: Postgraduate Program in Radiation, Minerals and Materials Science and Technology, CDTN; 2018

